



UNIVERSITY OF LEEDS

This is a repository copy of *New Development of Anodic Electro-catalyst for Chlor-alkali Industry*.

White Rose Research Online URL for this paper:
<http://eprints.whiterose.ac.uk/109190/>

Version: Accepted Version

Article:

Zafar, MS, Tausif, M orcid.org/0000-0003-0179-9013, ul-Haq, Z et al. (2 more authors) (2016) New Development of Anodic Electro-catalyst for Chlor-alkali Industry. *Portugaliae Electrochimica Acta*, 34 (4). pp. 257-266. ISSN 1647-1571

<https://doi.org/10.4152/pea.201604257>

This is an author produced version of a paper published in *Portugaliae Electrochimica Acta*. Uploaded in accordance with the publisher's self-archiving policy.

Reuse

Unless indicated otherwise, fulltext items are protected by copyright with all rights reserved. The copyright exception in section 29 of the Copyright, Designs and Patents Act 1988 allows the making of a single copy solely for the purpose of non-commercial research or private study within the limits of fair dealing. The publisher or other rights-holder may allow further reproduction and re-use of this version - refer to the White Rose Research Online record for this item. Where records identify the publisher as the copyright holder, users can verify any specific terms of use on the publisher's website.

Takedown

If you consider content in White Rose Research Online to be in breach of UK law, please notify us by emailing eprints@whiterose.ac.uk including the URL of the record and the reason for the withdrawal request.



eprints@whiterose.ac.uk
<https://eprints.whiterose.ac.uk/>

New development of anodic Electro-catalyst for Chlor-alkali industry

Muhammad Shahzad Zafar^{a*}, Muhammad Tausif^b, Zia-ul-Haq^c, Muhammad Ashraf^e, Sarfraz Hussain^e

^aDepartment of Chemical Engineering, University of Engineering and Technology (Faisalabad Campus) Lahore, Pakistan.

^bDepartment of Textile Engineering, University of Engineering and Technology (Faisalabad Campus) Lahore, Pakistan.

^cDepartment of Chemical Engineering, NFC Institute of Engineering & Fertilizer Research, Faisalabad, Pakistan.

*Corresponding Author

Email: shahzad.zafar@uet.edu.pk

Tel: +92 41 2433508

Fax: +92 41 2433501

Postal Address: University of Engineering and Technology, 3.5 km Khurrianwala, Mukoowana Bypass Road, Faisalabad, Pakistan

Abstract

Anodic Electro catalysts are developed by using a titanium substrate coated with different compositions of mixed oxides of ruthenium-titanium mixed oxides, ruthenium-titanium-tin mixed oxides and ruthenium-titanium-iridium mixed oxides. The performance of electro catalysts was further evaluated by measurement of coating thickness, studying coating morphology with microscope, identifying the presence of RuO₂, TiO₂, IrO₂ and SnO₂ in coating film and analyzing shape of individual crystal by XRD, performing accelerated life test and current efficiency test of selected anode. The coating composition of 15% RuO₂: 15% IrO₂ : 70% TiO₂ exhibited premium properties among studied anodes.

Keywords: Electrode, XRD, DSA, Accelerated Life Test, Titanium.

1. Introduction

Electro-catalyst enables the electron transfer reactions at the electrode-electrolyte interface with substantial energy savings. The total energy consumption in the chloro-alkali process is proportional to the total cell voltage, including thermodynamic potential of anodic and cathodic reactions, electrode over potential, ohmic drop from the electrolyte, membrane and bubble effect, etc. [1].

The electrode upon which oxidation occurs in an electrochemical cell is called “Anode”. The design and selection of the parameters of anodes have traditionally been associated to optimization of fixed and operating costs of the anode. Most of the materials used in anode

fabrication are characteristically expensive. However, higher costs are justified by enhanced performance and reduced operational cost. An additional consideration in the selection of an appropriate anode is that it should be environment-friendly.

Historically, graphite anodes were commonly employed in brine electrolysis industry. The use of these anodes was abandoned due to consumption of graphite anodes during the process. Moreover, the use of metal phosphides and metal disulfides as electro-catalysts in electrochemical cells, especially with alkaline electrolytes, was also a common practice [2-4].

Later on, the electro-catalysts based on Platinum and Nickel were developed and the brine electrolysis industry switched over to the use of these Dimensionally Stable Anodes (DSA) with subsequent industrial applications. The combination of innovative techniques like energy-saving membrane cell technology and DSA has since become the most preferred choice in the design and construction of new chlor-alkali industry [1, 5, 6]. DSA have the following main advantages compared to that of previously used graphite anodes:

- Lower power consumption
- Longer anode life
- Stability of electrodes during electrolysis
- Elimination of environmentally harmful materials
- Relatively consistent and stable cell room operation
- Reduction in labor.

Compact and crack-free coatings can be used as protective inner layer for the fabrication of DSA [7]. Hence, the DSA's are coated with expensive coating materials. The formulation of coating solution varies in each case while coating process parameters remain the same. Main types of DSA coatings used in electrochemical industries are:

- Ruthenium oxide based coating
- Iridium oxide based coatings
- Mixed ruthenium-iridium oxides coatings
- Platinum-Iridium coatings
- Ternary system of coatings

About 3 tons of Ruthenium per year (12% of the annual production of Ruthenium) is used for the fabrication of anodic electro-catalytic coatings [8]. Ruthenium based electro catalytic anodes they find applications in water electrolysis, electro-organic synthesis and electrochemical oxidation. [9-11]. Such types of anodes are used in caustic-chlorine cells, chlorate cells, sea water electrolysis and similar applications.

Technical innovation to improve the energy-efficiency and resource-efficiency in the chlor-alkali industry has become a critical issue in view of the current energy and environmental challenges being faced and the increasing shortages in the primary resources. [12] An attempt was made to reduce the electrode potential by about 100 mV (about 3–4% energy saving) and to reduce the ruthenium content [9-11].

The work presented in this paper aims to develop new anodic electro catalysts by using a titanium substrate, determine the optimum ruthenium oxide based electro catalytic coating composition and subject the specimen with optimized coating composition for current efficiency measurement to a pilot plant of capacity 1.3 kg of sodium chlorate per day.

2. Materials and Methods

In this experimental work, different ruthenium oxide based coatings for DSA were prepared followed by non-destructive testing (NDT) and electrochemical analysis to find out optimum coating composition. Both binary and ternary oxide systems were studied. Ruthenium-titanium mixed oxide coatings were investigated in binary systems (Type 1) whereas Iridium -Ruthenium and Titanium di-oxide and Ruthenium-Titanium and Stannic oxide coatings were investigated in ternary system (Type 2 and 3). Process parameters (chemical etching temperature and time, baking temperature and time, annealing temperature and time and loading of noble metals) for all types of coating compositions were kept fixed. The followed experimental design and the details of prepared specimen are depicted in Table 1.

- The performance of anodes was analyzed using Accelerated Life Test. In this technique, the test specimen of DSA was electrolyzed in saturated brine solution ($260\sim 290\text{ g l}^{-1}$ of NaCl) under constant current (operating current density 30 kA m^{-2}) and terminal voltage. The brine solution was circulated by a sealed pump in order to keep the composition of solution uniform. The pH of solution was maintained between 6~7. The voltage across the working and reference electrodes were recorded until the voltage increased sharply and test specimen broke down. In Accelerated Life Test, the cell voltage slowly decreases at first (caused by the activation of the inner surface in the porous anode), then the voltage remain unchanged for a long period of time and finally steeply decreases at the end of specimen's service life. The specimen with highest accelerated life time was further subjected to Current Efficiency Measurement test.
-

Table 1: Details of prepared Specimens

Coating Type	Specimen #	Coating composition	# of coats applied	Chemical Formulae
1	1A 1B	Ruthenium-Titanium mixed oxides	10	RuO_2 TiO_2
2	2A 2B	Ruthenium-Titanium-Tin mixed oxides	12	RuO_2 TiO_2 SnO_2
3	3A 3B	Ruthenium-Titanium-Iridium mixed oxides.	10	RuO_2 TiO_2 IrO_2

2.1 Process Description

The coating process of DSA comprised of following five stages and the process flow chart is provided in Figure 1.

1. Preparation of titanium substrate
2. Application of coating solution to substrate
3. Baking of coated substrate
4. Annealing of specimen
5. Inspection of coated anodes

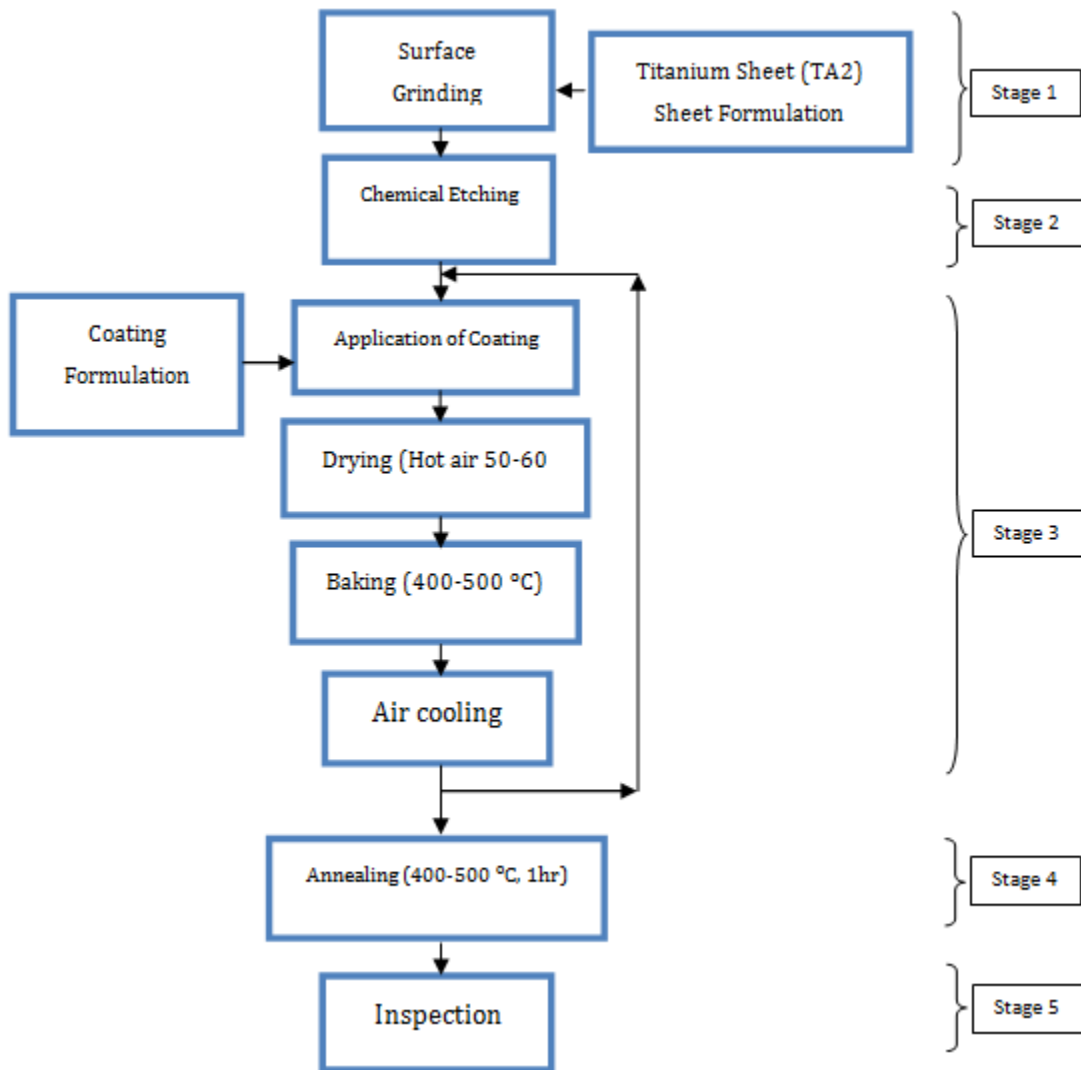


Figure 1: Flow chart of the coating process of DSA

2.1.1 Preparation of Substrate

A specimen of titanium sheet (Chinese standard:TA2) having grain size 25~55 μm was selected. The sheet was ground with sand paper for the removal of foreign matter. For verification of grain size, metallography of titanium sheet was performed with the aid of an optical metallurgical microscope. Typical micrographs, for 3B (having grain size of 54 micro-meters) and 2B (having grain size of 46 micro-meters), are shown in Figure 2. The ground specimen was etched for three hours with oxalic acid (10% w/w) at 80⁰C. The results of morphology for different specimen are depicted in Table 2.

Table 2: Prepared Metallograph with their grain sizes

Coating Type	Specimen #	Grain size (μm)
1	1A	27
	1B	28
2	2A	45
	2B	46
3	3A	53
	3B	54

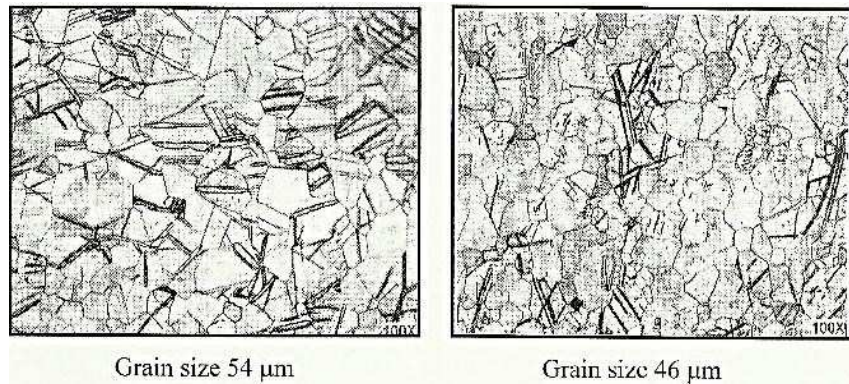


Figure 2: Typical metallograph of grain size 54 μm and 46 μm

2.1.2 Application of coating solution to substrate

The surface of specimens was painted with a coating solution, formulations are given in Table 3.

Table 3: Details of prepared Specimens

Specimen #	Coating Composition (mole %)	# of Coats Applied	Loading
1A	RuO ₂ = 30 %	10	Ru 4.5 g/m ²
1B	TiO ₂ = 70 %		5.1 g/m ²
2A	RuO ₂ = 16.65 %	12	RuO ₂ + SnO ₂ 1.37 g/ft ² 1.51 g/ft ²
2B	TiO ₂ = 66.70 %		
	SnO ₂ = 16.65 %		
3A	RuO ₂ = 15 %	10	Ru + Ir 6.97 g/m ² 7.96 g/m ²
3B	TiO ₂ = 70 %		
	IrO ₂ = 15 %		

2.1.3 Baking of painted substrate

The painted specimens were dried with hot air at 50~60°C. The suitable thermal sintering temperature for the fabrication of anodic coatings is between 400–550°C. The dried specimens were baked in presence of excess air at 450°C in a furnace for 10 minutes. Higher temperatures (> 550 °C) can result in the partial oxidation of the Ti substrate [13], which is likely to increase the ohmic resistance of the oxide film due to the formation of insulating TiO_x interlayer. Thereafter, the specimen were cooled and painted again. The process of painting, drying, baking, and cooling was repeated until desired thickness of ruthenium metal was obtained.

2.1.4 Annealing

Finally the specimens were heated at temperature of 450°C for one hour and were gradually cool down to ambient temperature. This process is called “Annealing”. It induces ductility, soften the material, relieve internal stresses, refine the structure by making it homogeneous, and improve the cold working properties. Details of prepared specimens are given in Table 3 above.

2.1.5 Inspection of Coated Anodes

The inspection of anodes was carried out in order to determine coating quality, material identifications and performance of anode. The coated specimens were inspected with optical metallurgical microscope for the verification of coating morphology and measurements of coating thickness. The coated specimens were also inspected for the identification of compounds\elements and for the study of crystal structure with XRD.

3. Results

The results are tabulated, graphically reported and critically discussed as:

3.1 Coating Morphology

Coating morphology can affect the electrode performance such as the available active surface area, electrode deactivation due to the passivation [14] and also the gas bubble evolution behavior during the process [15].

Typical micrographs of different anodes are shown in Figure 3. All the three micrographs show a characteristic micro-cracked surface. These cracks have occurred early in the coating because solvent evaporated from the surface and left a gel of un reacted Ruthenium, Iridium, Tin and Titanium compounds. Further, as the coating was baked at higher temperatures, these cracks increased in size because of the volume contraction of the gel [16]. The establishment of cracks caused the increase in surface area compared to that of geometrical area.

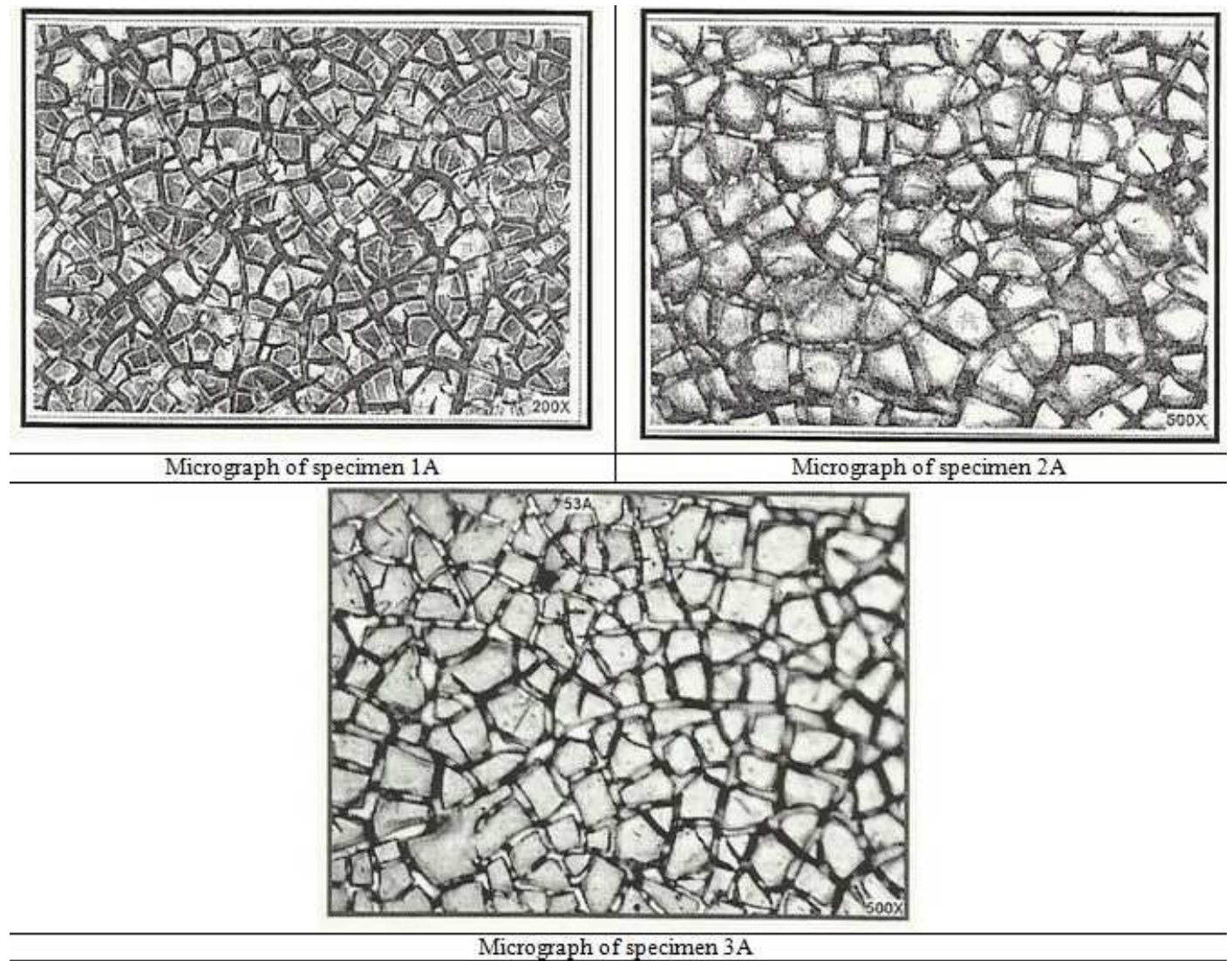


Figure 3: Micrographs of specimen having grain size of 27 μm (1A), 45 μm (2A) and 53 μm (3A)

The increase in surface area contributes to low chlorine discharge potential of these coatings and hence can provides a large number of catalytic sites for gas evolution while minimizing concentration polarization.

3.2 Coating Thickness

The coating thickness of different specimens was measured by using optical metallurgical microscope. Thickness in micro-meters are presented in Table 4 and micrographs of some typical specimen are shown in Figure 4:

Table 4 Coating thickness of speciemen

Specimen #	Coating Composition (mole %)	Thickness (μm)
1B	RuO ₂ = 30 %	14.63
	TiO ₂ = 70 %	
2B	RuO ₂ = 16.65 %	4.8
	TiO ₂ = 66.70 %	
	SnO ₂ = 16.65 %	
3B	RuO ₂ = 15 %	6.3
	TiO ₂ = 70 %	
	IrO ₂ = 15 %	

The speciemen coated by a binary oxide system, i.e. mixed oxides of ruthenium-titanium has the highest coating thickness. It may be due to the presence of high concentration of Ruthenium dioxide but the trend is less steeply observed handling the ternary oxide systems. However, in ternary oxide systems, the presence of Iridium improves the coating thickness as compared to the thickness achieved by using tin mixed oxides.

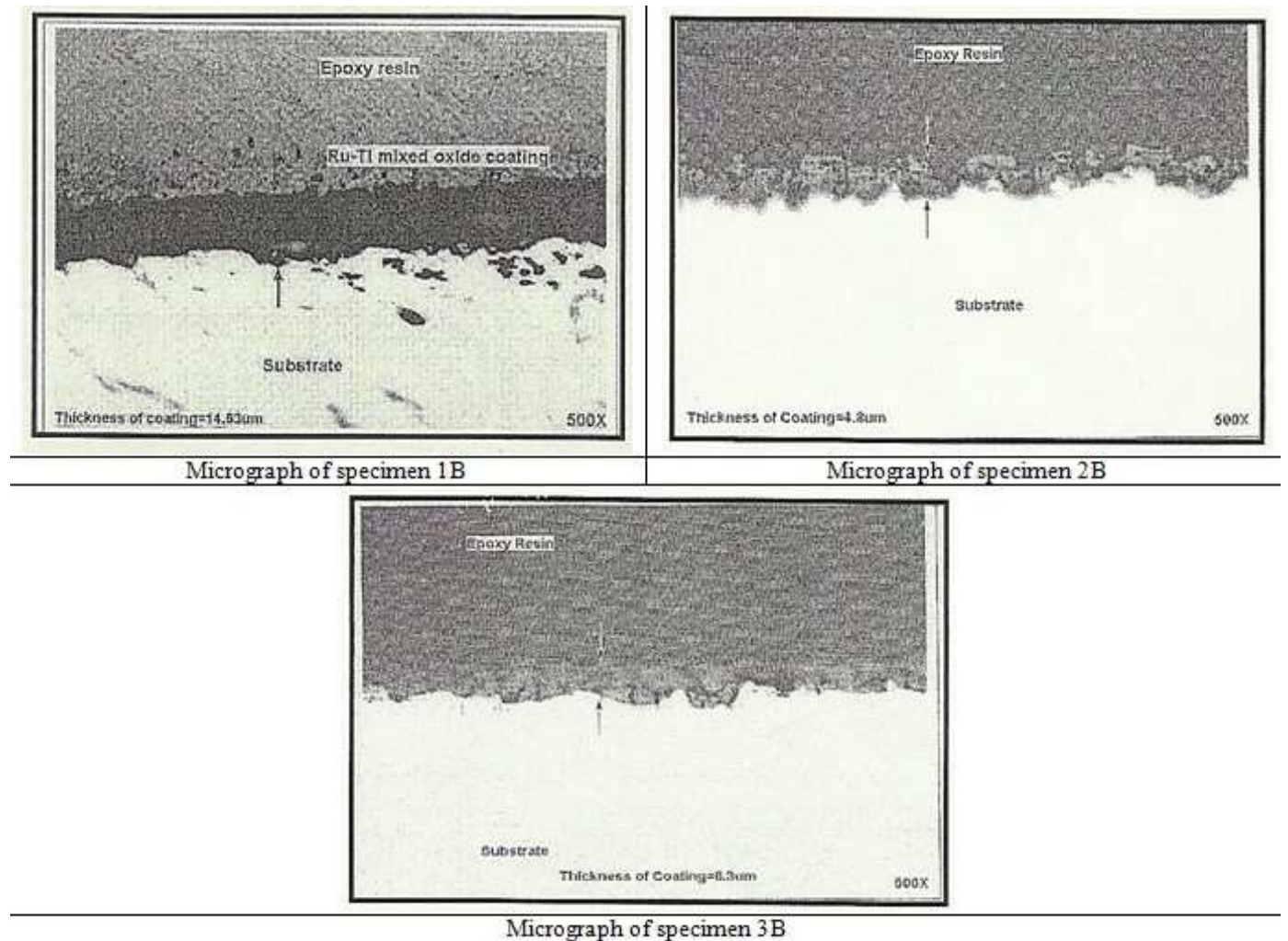


Figure 4: Micrographs of specimen having grain size of 28 μm (1B), 46 μm (2B) and 54 μm (3B)

3.3 Identification of Elements and Compounds

Different specimens were analyzed by X-ray diffractometer for the identification of elements and compounds in coating solution and for the study of structure of solid solution. XRD peaks of different specimens are shown in Figure 5. It is clear that the specimen 1B, possessing the larger peaks have high concentration of titanium on its surface.

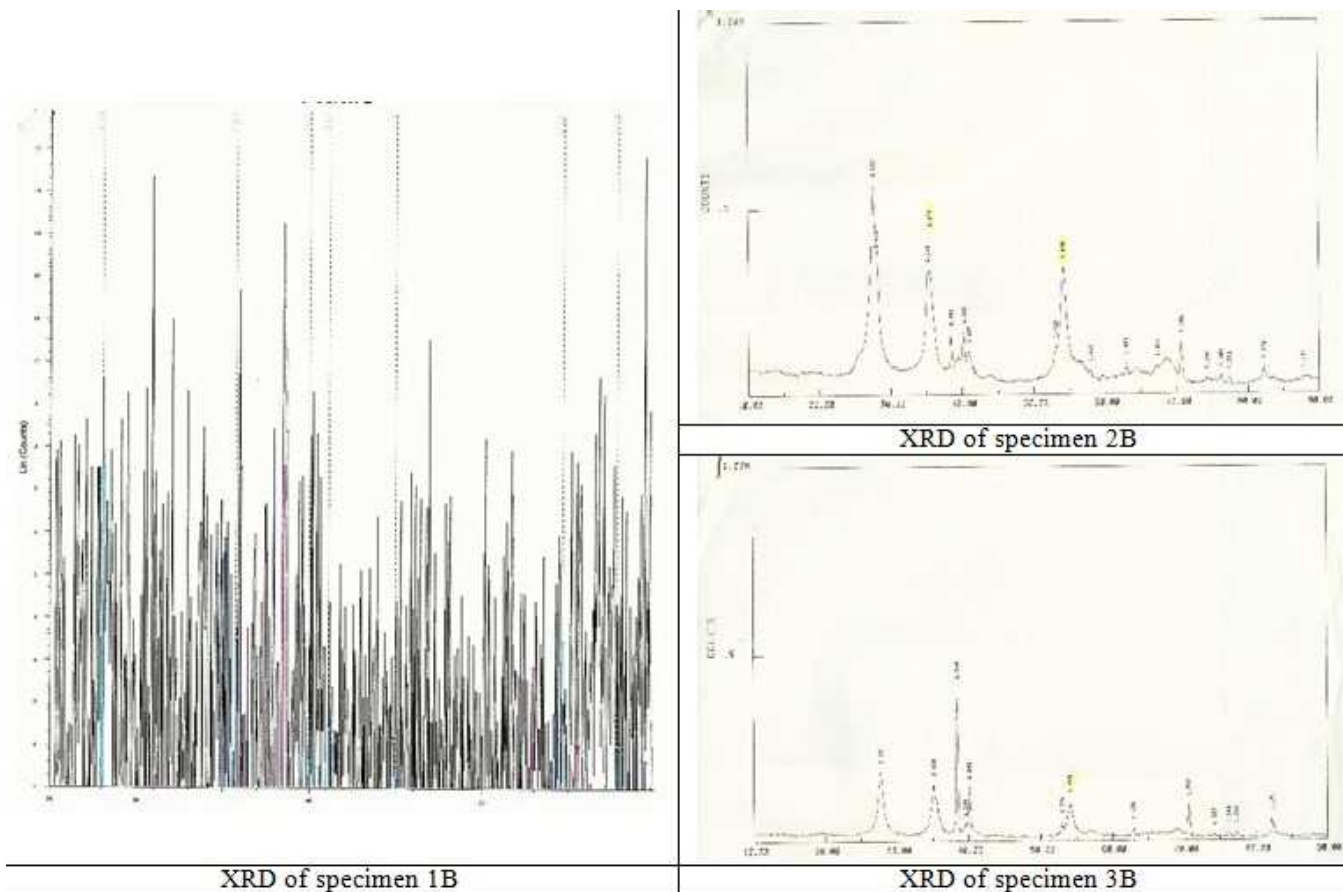


Figure 5: XRD peaks of specimen having grain size of 28 μm (1B), 46 μm (2B) and 54 μm (3B)
 The compounds and elements present in the coatings of the three specimens identified by the XRD technique are given in Table 5.

Table 5: Identification of Compounds and Elements in Coatings by XRD Technique

Specimen #	Compounds	Elements
1B	Ruthenium dioxide Titanium dioxide Titanium dioxide	Titanium
2B	Ruthenium dioxide Titanium dioxide Stannic oxide	Titanium
3B	Ruthenium dioxide Titanium dioxide Iridium oxide	Titanium

3.4 Performance of Anode

Accelerated Life Test and Current Efficiency Measurement techniques were used to evaluate the performance of anodes.

3.4.1 Accelerated Life Test

The continuous tests stimulating industrial conditions employing operating current density of 3 kA m^{-2} would certainly provide reliable data on anode durability but would require 2-3 years per test. Keeping this fact in view, the procedure was modified during the experimentation by operating the test anode at a high current density (30 kA m^{-2}) at room temperature in dilute brine (30 g l^{-1}). The brine is circulated by a sealed pump in order to keep the composition of solution uniform and the pH of solution is also maintained between 6~7. These conditions give a potential voltage, i.e. greater than the critical value of 1.4 V, where corrosion of coating occurs within a few hours. The result of this test is shown in Figure 6, which depicts that that specimen # 53 has maximum life among the studied specimens.

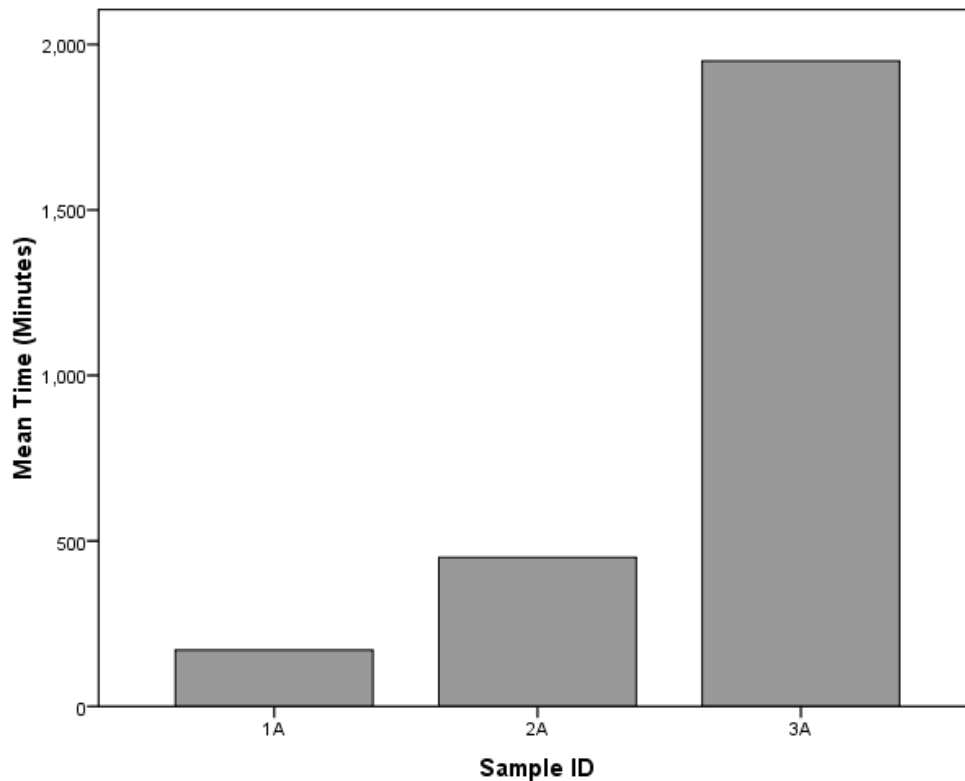


Figure 6: Accelerated Life Test

3.4.2 Current Efficiency Measurement

The fabricated anode was installed in a pilot plant of sodium chlorate with capacity of 1.3 kg per day. The plant was operated at the same current density as in actual operation (2.2 kA m^{-2} , 85°C). After operating the plant for 34 hours, the current efficiency was found to be 94.2 % (Table 6).

Table 6: Current Efficiency of sodium chlorate (by Faraday Laws of electrolysis)

Production of Sodium Chlorate (g)		Current Efficiency (%)
Theoretical	Actual	
1848	1742	94.2

4 Conclusions:

Ruthenium oxide based coatings on titanium are known to produce dimensionally stable anodes. The effect of coating types, number of coats and coating composition on the Accelerated Life of titanium anodes was experimentally studied. It was concluded that a ternary oxide system having Iridium-Ruthenium and Titanium di-oxide coating, with the coating composition of 15% RuO₂, 70% TiO₂ and 15% IrO₂, exhibited longest Accelerated Life among studied specimens and showed a current efficiency of 94.2 %. Hence, the life of titanium anode could be prolonged by employing a ternary oxide system having a moderate coating thickness of 6.3 μm to inhibit corrosion. It is likely to have economical as well as environmental benefits by slow depletion of anodes which are manufactured from finite natural resources.

References:

1. Trasatti, S., *Physical electrochemistry of ceramic oxides*. Electrochimica acta, 1991. **36**(2): p. 225-241.
2. Mund, K. and R. Schulte, *Electro-catalyst and process of manufacture*. 1976, Google Patents.
3. Larson, T.L., *METHOD OF PRODUCING A FUEL CELL ELEC-TRODE CONTAINING A NICKEL-PHOSPHORUS ALLOY AS THE CATALYST*. 1968, Google Patents.
4. Hills, B., *ELECTRODE COMPRISING NON-NOBLE METAL DISULFIDES OR PHOSPHIDES AND ELECTRO-CHEMICAL CELL UTILIZING SAME*. 1971, Google Patents.
5. Beer, H.B., *The invention and industrial development of metal anodes*. Journal of the Electrochemical Society, 1980. **127**(8): p. 303C-307C.
6. Beer, H.B., in *British Patent*. 1965: British.
7. Chen, R., V. Trieu, H. Natter, et al., *In situ Supported Nanoscale Ru x Ti1- x O2 on Anatase TiO2 with Improved Electroactivity*. Chemistry of Materials, 2010. **22**(23): p. 6215-6217.
8. Zhou, H.-C., J.R. Long, and O.M. Yaghi, *Introduction to metal-organic frameworks*. Chemical reviews, 2012. **112**(2): p. 673-674.
9. Kim, K.-W., Y.-J. Kim, I.-T. Kim, et al., *The electrolytic decomposition mechanism of ammonia to nitrogen at an IrO₂ anode*. Electrochimica acta, 2005. **50**(22): p. 4356-4364.
10. Chiang, L.-C., J.-E. Chang, and T.-C. Wen, *Indirect oxidation effect in electrochemical oxidation treatment of landfill leachate*. Water Research, 1995. **29**(2): p. 671-678.
11. Reichert, E., R. Wintringer, D.A. Volmer, et al., *Electro-catalytic oxidative cleavage of lignin in a protic ionic liquid*. Physical Chemistry Chemical Physics, 2012. **14**(15): p. 5214-5221.
12. Ostertag, K., C. Sartorius, and L. Tercero Espinoza, *Innovationsdynamik in rohstoffintensiven Produktionsprozessen*. Chemie Ingenieur Technik, 2010. **82**(11): p. 1893-1901.

13. Martelli, G., R. Ornelas, and G. Fajta, *Deactivation mechanisms of oxygen evolving anodes at high current densities*. *Electrochimica acta*, 1994. **39**(11): p. 1551-1558.
14. Chen, R., V. Trieu, A.R. Zeradjanin, et al., *Microstructural impact of anodic coatings on the electrochemical chlorine evolution reaction*. *Physical Chemistry Chemical Physics*, 2012. **14**(20): p. 7392-7399.
15. Chen, R., V. Trieu, H. Natter, et al., *Wavelet analysis of chlorine bubble evolution on electrodes with different surface morphologies*. *Electrochemistry Communications*, 2012. **22**: p. 16-20.
16. Kozuka, H., M. Kajimura, T. Hirano, et al., *Crack-free, thick ceramic coating films via non-repetitive dip-coating using polyvinylpyrrolidone as stress-relaxing agent*. *Journal of Sol-Gel Science and Technology*, 2000. **19**(1-3): p. 205-209.

Figures:

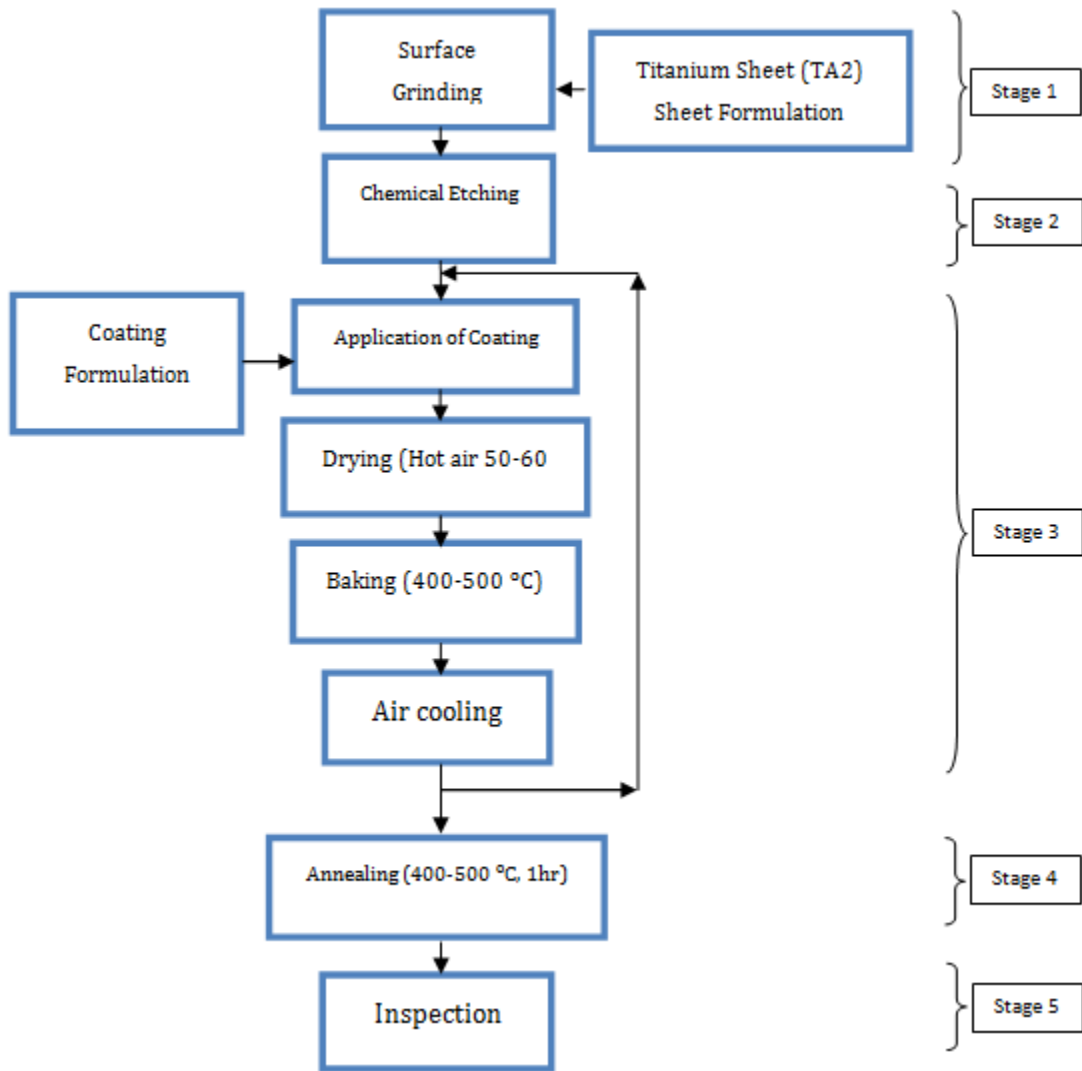


Figure 3: Flow chart of the coating process of DSA

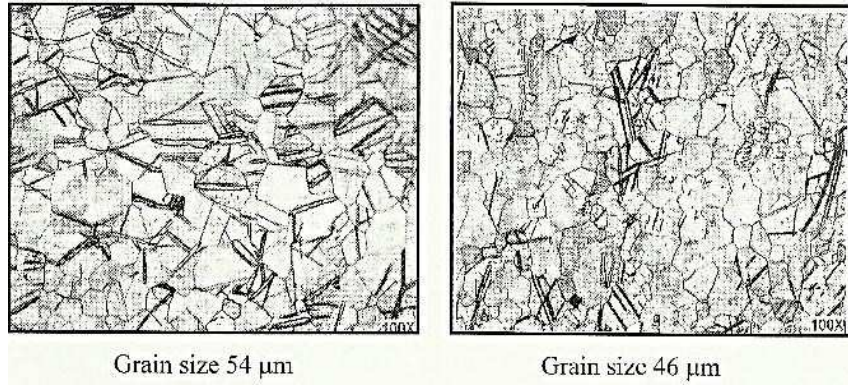
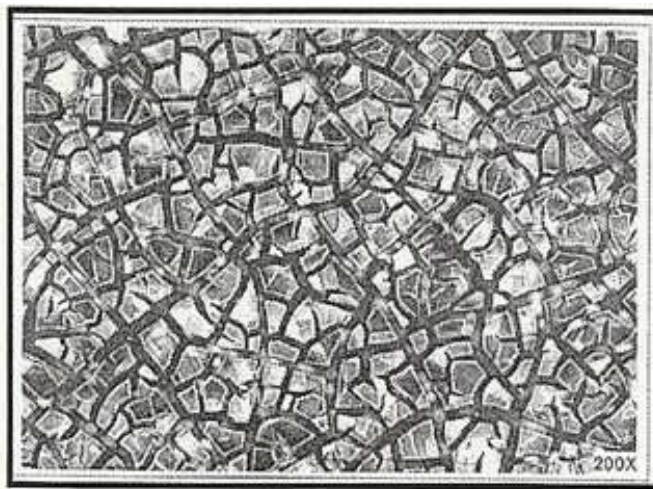
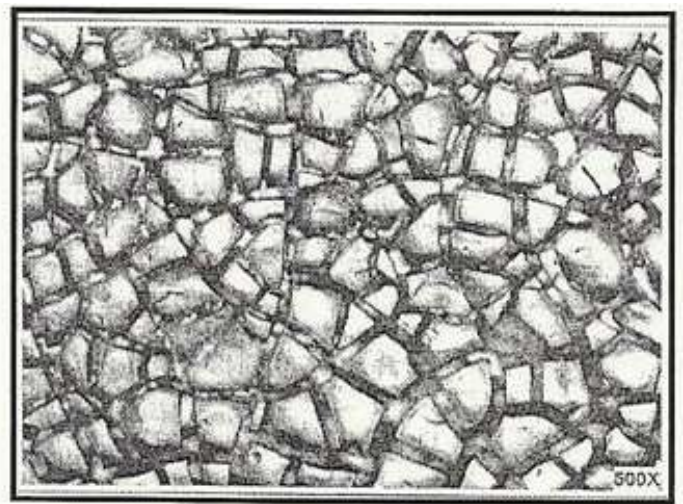


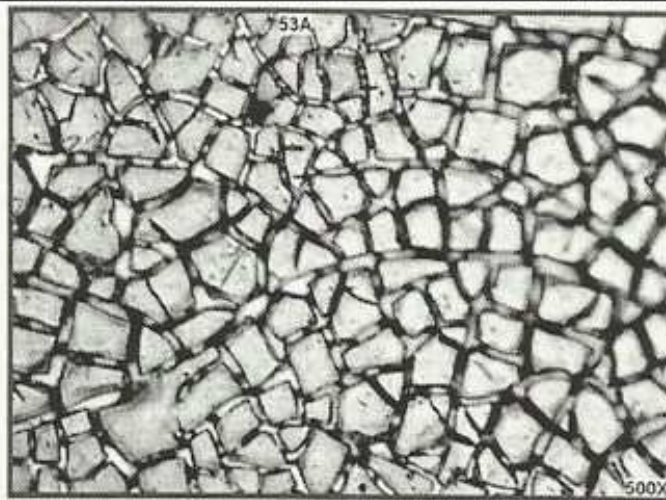
Figure 4: Typical metallograph of grain size 54 μm and 46 μm



Micrograph of specimen 1A

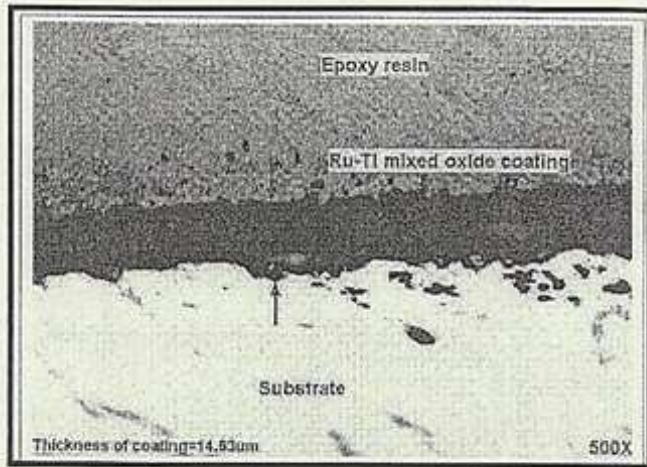


Micrograph of specimen 2A

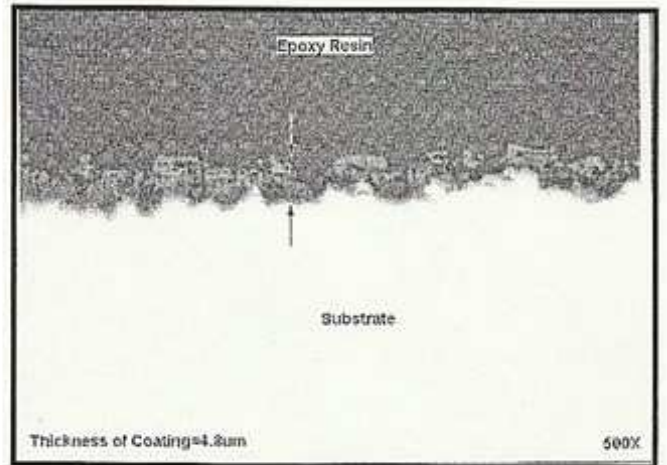


Micrograph of specimen 3A

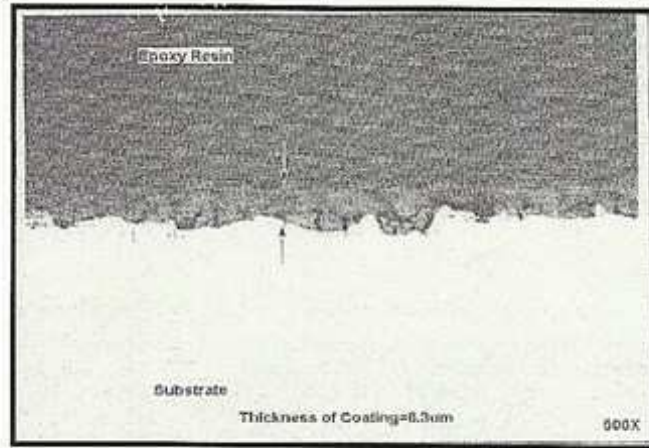
Figure 3: Micrographs of specimen having grain size of 27 μm (1A), 45 μm (2A) and 53 μm (3A)



Micrograph of specimen 1B

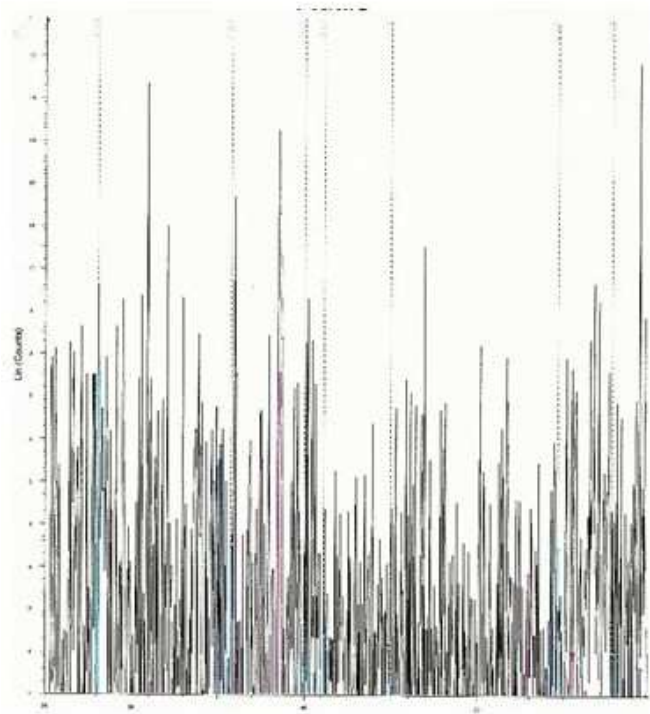


Micrograph of specimen 2B

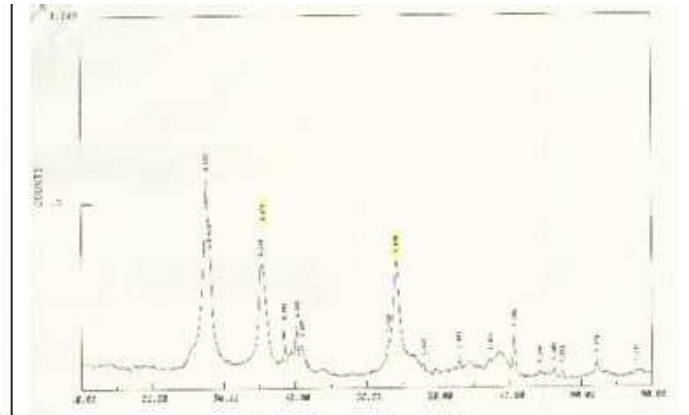


Micrograph of specimen 3B

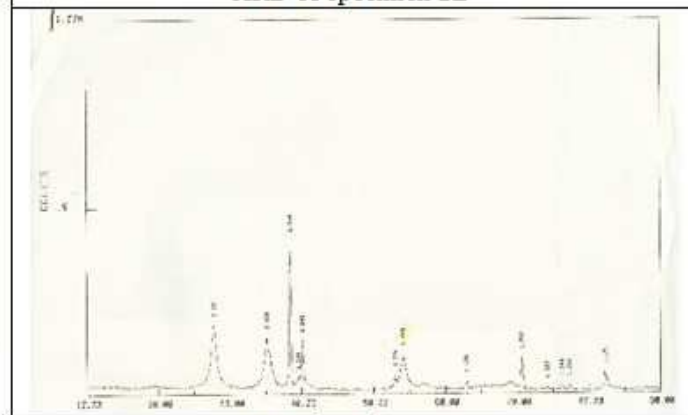
Figure 4: Micrographs of specimen having grain size of 28 μm (1B), 46 μm (2B) and 54 μm (3B)



XRD of specimen 1B



XRD of specimen 2B



XRD of specimen 3B

Figure 5: XRD peaks of specimen having grain size of 28 μm (1B), 46 μm (2B) and 54 μm (3B)

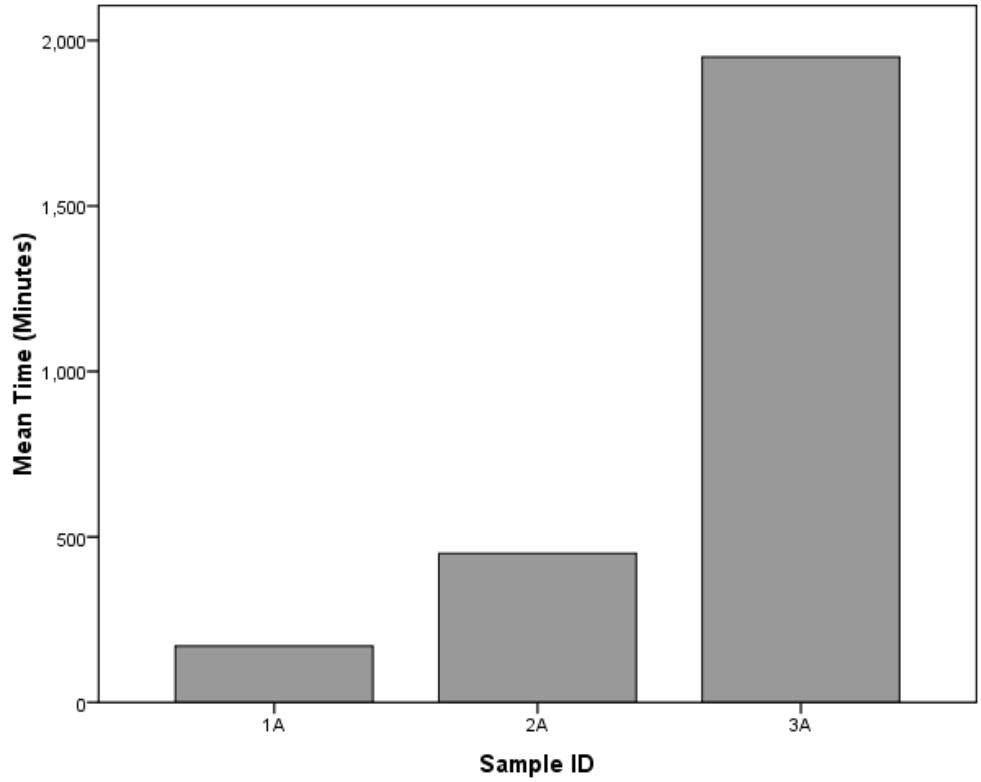


Figure 6: Accelerated Life Test